

Article

## Effects of Fe<sub>3</sub>O<sub>4</sub> Magnetic Nanoparticles on A549 Cells

Masatoshi Watanabe <sup>1,\*</sup>, Misao Yoneda <sup>2</sup>, Ayaka Morohashi <sup>1</sup>, Yasuki Hori <sup>1</sup>, Daiki Okamoto <sup>1</sup>, Akiko Sato <sup>1</sup>, Daisuke Kurioka <sup>1</sup>, Tadashi Nittami <sup>1</sup>, Yoshifumi Hirokawa <sup>2</sup>, Taizo Shiraishi <sup>2</sup>, Kazuaki Kawai <sup>3</sup>, Hiroshi Kasai <sup>3</sup> and Yukari Totsuka <sup>4</sup>

<sup>1</sup> Laboratory for Medical Engineering, Division of Materials and Chemical Engineering, Graduate School of Engineering, Yokohama National University, Yokohama 240-8501, Japan; E-Mails: qqmoro@gmail.com (A.M.); c17cssbos@gmail.com (Y.H.); dokamoto615@yahoo.co.jp (D.O.); akko.613@gmail.com (A.S.); kuri321@gmail.com (D.K.); nittami@ynu.ac.jp (T.N.)

<sup>2</sup> Department of Pathologic Oncology, Institute of Molecular and Experimental Medicine, Mie University Graduate School of Medicine, Tsu 514-8507, Japan; E-Mails: xyxfp209@yahoo.co.jp (M.Y.); ultray2k@clin.medic.mie-u.ac.jp (Y.H.); tao@doc.medic.mie-u.ac.jp (T.S.)

<sup>3</sup> Department of Environmental Oncology, Institute of Individual Ecological Sciences, University of Occupational and Environmental Health, Kitakyushu 807-8555, Japan; E-Mails: kkawai@med.uoeh-u.ac.jp (K.K.); h-kasai@med.uoeh-u.ac.jp (H.K.)

<sup>4</sup> Division of Cancer Development System, National Cancer Center Research Institute, Tokyo 104-0045, Japan; E-Mail: ytotsuka@gan2.res.ncc.go.jp

\* Author to whom correspondence should be addressed; E-Mail: mawata@ynu.ac.jp; Tel./Fax: +81-45-339-3997.

Received: 8 June 2013; in revised form: 8 July 2013 / Accepted: 18 July 2013 /

Published: 25 July 2013

---

**Abstract:** Fe<sub>3</sub>O<sub>4</sub> magnetic nanoparticles (MgNPs-Fe<sub>3</sub>O<sub>4</sub>) are widely used in medical applications, including magnetic resonance imaging, drug delivery, and in hyperthermia. However, the same properties that aid their utility in the clinic may potentially induce toxicity. Therefore, the purpose of this study was to investigate the cytotoxicity and genotoxicity of MgNPs-Fe<sub>3</sub>O<sub>4</sub> in A549 human lung epithelial cells. MgNPs-Fe<sub>3</sub>O<sub>4</sub> caused cell membrane damage, as assessed by the release of lactate dehydrogenase (LDH), only at a high concentration (100 µg/mL); a lower concentration (10 µg/mL) increased the production of reactive oxygen species, increased oxidative damage to DNA, and decreased the level of reduced glutathione. MgNPs-Fe<sub>3</sub>O<sub>4</sub> caused a dose-dependent increase in the

CD44<sup>+</sup> fraction of A549 cells. MgNPs-Fe<sub>3</sub>O<sub>4</sub> induced the expression of heme oxygenase-1 at a concentration of 1 µg/mL, and in a dose-dependent manner. Despite these effects, MgNPs-Fe<sub>3</sub>O<sub>4</sub> had minimal effect on cell viability and elicited only a small increase in the number of cells undergoing apoptosis. Together, these data suggest that MgNPs-Fe<sub>3</sub>O<sub>4</sub> exert little or no cytotoxicity until a high exposure level (100 µg/mL) is reached. This dissociation between elevated indices of cell damage and a small effect on cell viability warrants further study.

**Keywords:** magnetic nanoparticles; cytotoxicity; genotoxicity; A549; CD44

---

## 1. Introduction

Nanotechnology—the manipulation and production of matter sized between 1 and 100 nm—has grown markedly with the promise of substantial benefits and applicability to such diverse areas as clothing, electronics, engineering, and healthcare [1]. The principal goal of nanotechnology is to develop new materials in the nanometer scale, including nanoparticles, defined as particulate materials with at least one dimension of less than 100 nm. The design and development of nanomaterials have been of fundamental importance to the industry, given their novelty and the benefits conferred by their physicochemical properties.

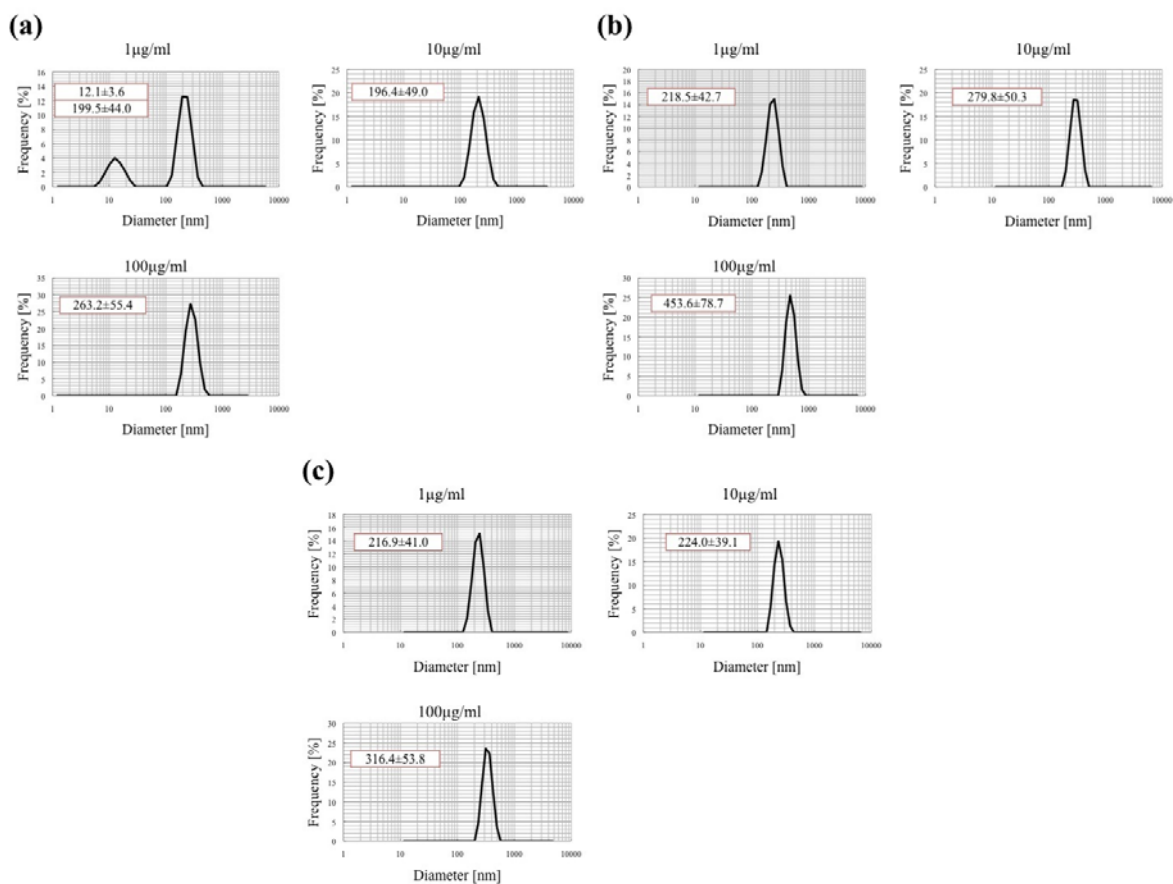
Magnetic nanoparticles (MgNPs) are a subclass of nanomaterials. Among MgNPs, Fe<sub>3</sub>O<sub>4</sub>-containing MgNPs (MgNP-Fe<sub>3</sub>O<sub>4</sub>; magnetite) are the only MgNPs approved for clinical use. Magnetite has a cubic inverse spinel structure with oxygen forming a face-centered cubic (FCC) closed packing; the interstitial tetrahedral and octahedral sites are occupied by Fe cations [2]. Due to their unique physical, chemical, and mechanical features, MgNPs-Fe<sub>3</sub>O<sub>4</sub> have been used as magnetic resonance imaging contrast agents, targeted drug delivery systems, and hyperthermic agents when placed in an external magnetic field [3,4]. Modified/unmodified MgNP-Fe<sub>3</sub>O<sub>4</sub> has been reported to improve the efficiency of anticancer drugs and reverse multidrug resistance [5,6]. However, these same properties of MgNPs can induce cytotoxicity and genotoxicity [7]. Studies have shown that MgNPs-Fe<sub>3</sub>O<sub>4</sub> are less toxic than MgNPs containing SiO<sub>2</sub>, TiO<sub>2</sub>, CuO, and TiO<sub>2</sub> [7–9]. However, results regarding the potential of MgNPs-Fe<sub>3</sub>O<sub>4</sub> to induce cytotoxicity, genotoxicity, and oxidative stress, have been inconsistent [7–11], necessitating further study to identify any potential toxicity associated with their use. Therefore, the objective of this study was to investigate the cytotoxicity and genotoxicity of MgNPs-Fe<sub>3</sub>O<sub>4</sub>. Experiments were designed to examine the effect of MgNPs-Fe<sub>3</sub>O<sub>4</sub> on indices of oxidative stress, and resultant cellular and nuclear damage in A549, human alveolar epithelial-like type-II cells. We also assessed the effect of MgNPs-Fe<sub>3</sub>O<sub>4</sub> on the expression of CD44, a transmembrane glycoprotein involved in inflammation, cell migration, signaling, and tumor metastasis [12,13].

## 2. Results and Discussion

Studies regarding the toxicological impact of MgNPs-Fe<sub>3</sub>O<sub>4</sub> have yielded disparate results, depending on the cell type, surface modification, cell medium composition, protein-MgNP interaction,

and oxidation state of iron [7,14]. We evaluated the cytotoxic effects of MgNPs-Fe<sub>3</sub>O<sub>4</sub> in A549 cells. We report that MgNPs-Fe<sub>3</sub>O<sub>4</sub> caused LDH leakage only at a concentration of 100 µg/mL; increased ROS production and 8-OH-dG content, and decreased glutathione (GSH) levels were found with 10 µg/mL MgNPs-Fe<sub>3</sub>O<sub>4</sub>. Despite these responses, MgNPs-Fe<sub>3</sub>O<sub>4</sub> caused only a small decrease and increase in cell viability and apoptosis, respectively.

**Figure 1.** Measurement of MgNPs-Fe<sub>3</sub>O<sub>4</sub> size by dynamic light scattering. MgNPs-Fe<sub>3</sub>O<sub>4</sub> were suspended at a concentration of 1, 10 or 100 µg/mL in (a) Ham's F-12 Medium with 10% fetal bovine serum (FBS); (b) Ham's F-12 Medium alone; (c) Phosphate-buffered saline (PBS).



### 2.1. Characterization of MgNPs-Fe<sub>3</sub>O<sub>4</sub> Suspension in Various Conditioned Medium

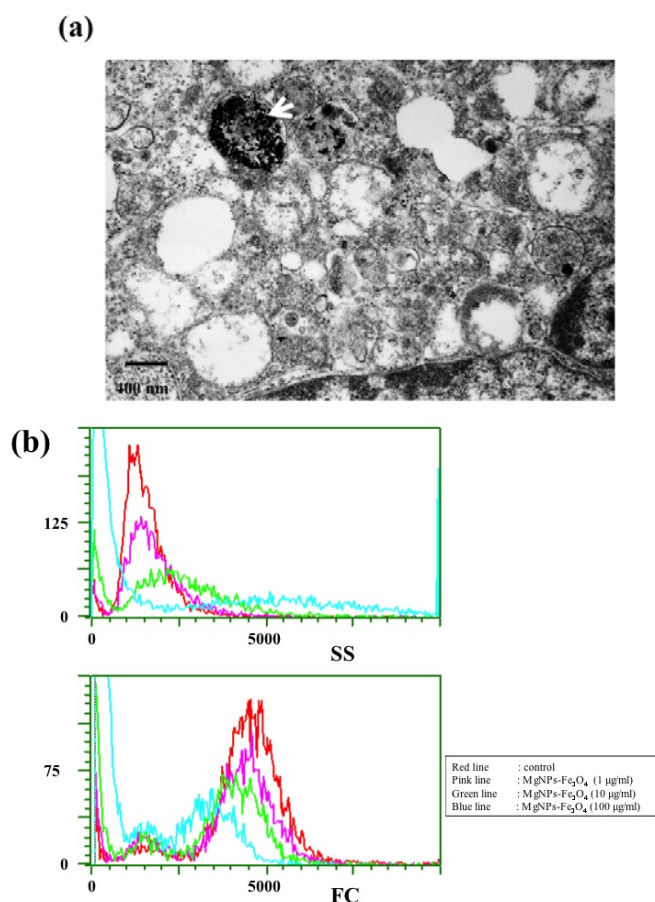
One of the most important significant factors for analysis of the toxicity of nanoparticles is size. As well as the sizes of the primary nanoparticles, the hydrodynamic sizes of secondary nanoparticles in dispersion are important as their sizes have a dramatic effect on cell response to exposure. The high ionic nature of the solution and the electrostatic/van der Waals interaction between protein and nanoparticles results in the formation of secondary particles. The mean hydrodynamic diameter of MgNPs-Fe<sub>3</sub>O<sub>4</sub> in Ham's F-12 medium, without FBS or supplements, increased in a dose-dependent manner (Figure 1b). In Ham's F-12 medium with 10% FBS and supplements or PBS, the mean hydrodynamic diameter was comparable between MgNP-Fe<sub>3</sub>O<sub>4</sub> suspensions of 1 and 10 µg/mL (Figure 1a,c); mean hydrodynamic diameter of MgNPs-Fe<sub>3</sub>O<sub>4</sub> was greater at 100 µg/mL in both media.

Together, these data suggest that MgNPs-Fe<sub>3</sub>O<sub>4</sub> agglomerate at a high concentration. The presence of FBS appeared to enhance the stability of MgNPs-Fe<sub>3</sub>O<sub>4</sub> in suspension. These data are consistent with a previous report showing that MgNPs show increased stability against aggregation in the RPMI-1640 with an increasing amount of FBS [15]. Therefore, the influence by the sedimentation rate of the secondary nanoparticles (NPs) and ratios of protein to NPs could be taken into consideration in the *in vitro* toxicity of NPs. These results shows the hydrodynamic sizes of secondary nanoparticles in Ham's F-12 medium with 10% FBS used in this study.

## 2.2. MgNPs-Fe<sub>3</sub>O<sub>4</sub> Uptake

A representative micrograph shows that after 24 h, MgNPs-Fe<sub>3</sub>O<sub>4</sub> aggregate within intracellular vesicles in A549 cells (Figure 2a). Figure 2b shows the flow cytometric light scatter histograms of the cells treated with the 0, 1, 10, or 100 µg/mL MgNPs-Fe<sub>3</sub>O<sub>4</sub>. The forward-scattered (FS) intensity (reflective of cell size) did not change; conversely, side-scattered (SS) intensity (reflective cellular uptake) increased in a dose-dependent manner. That is, the cells, which took up higher doses of MgNPs showed higher intensities of SS.

**Figure 2.** MgNPs-Fe<sub>3</sub>O<sub>4</sub> uptake in A549 cells; **(a)** Transmission electron microscopy imaging of A549 cells treated with 10 µg/mL Fe<sub>3</sub>O<sub>4</sub> magnetic nanoparticles (MgNPs-Fe<sub>3</sub>O<sub>4</sub>) for 24 h. MgNPs-Fe<sub>3</sub>O<sub>4</sub> are enclosed in vesicles (arrow); **(b)** Analysis of MgNPs-Fe<sub>3</sub>O<sub>4</sub> uptake by flow cytometric light scatter. A549 cells were treated with 0 (control), 1, 10 or 100 µg/mL MgNPs-Fe<sub>3</sub>O<sub>4</sub> for 24 h. SS: side-scattered; FS: forward-scattered.



### 2.3. Effect of MgNPs-Fe<sub>3</sub>O<sub>4</sub> on Cell Viability, Cell Membrane Damage, and Apoptosis

Treatment with MgNPs-Fe<sub>3</sub>O<sub>4</sub> for 24 h did not affect cell viability as assessed by the Alamar Blue assay. However, treatment with 100 µg/mL MgNPs-Fe<sub>3</sub>O<sub>4</sub> for 72 h caused a significant reduction in cell viability (Figure 3). Significant LDH leakage was detected following treatment with 100 µg/mL MgNPs-Fe<sub>3</sub>O<sub>4</sub>; lower concentrations had no effect (Figure 4). As shown in Figure 5a, treatment with 100 µg/mL MgNPs-Fe<sub>3</sub>O<sub>4</sub> for 24 h caused a small but significant increase in the percentage Annexin V-staining cells; however, these values were greatly below that caused by H<sub>2</sub>O<sub>2</sub> (Figure 5b).

**Figure 3.** Effect of Fe<sub>3</sub>O<sub>4</sub> magnetic nanoparticles (MgNPs-Fe<sub>3</sub>O<sub>4</sub>) on viability of A549 cells. A549 cells were treated with 0 (control), 1, 10 or 100 µg/mL MgNPs-Fe<sub>3</sub>O<sub>4</sub> for 24 or 72 h. Cell viability was assessed using the Alamar Blue assay. Data are presented as the mean ± SD of 3 independent experiments. \*  $p < 0.05$  vs. control.

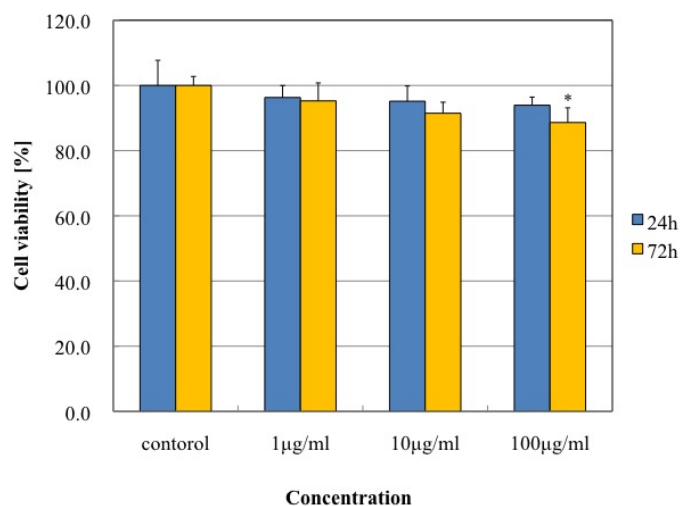


**Figure 4.** Effect of MgNPs-Fe<sub>3</sub>O<sub>4</sub> on lactate dehydrogenase (LDH) release by A549 cells. A549 cells were treated with 0 (control), 1, 10 or 100 µg/mL MgNPs-Fe<sub>3</sub>O<sub>4</sub> for 24 h. LDH release was assessed by formazan absorbance (LDH Cytotoxicity Assay Kit). Data are presented as the mean ± SD of 3 independent experiments. \*\*  $p < 0.01$  vs. control.

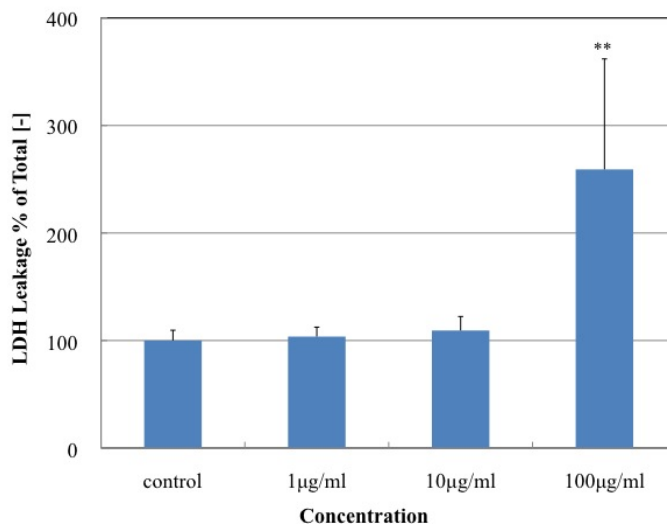
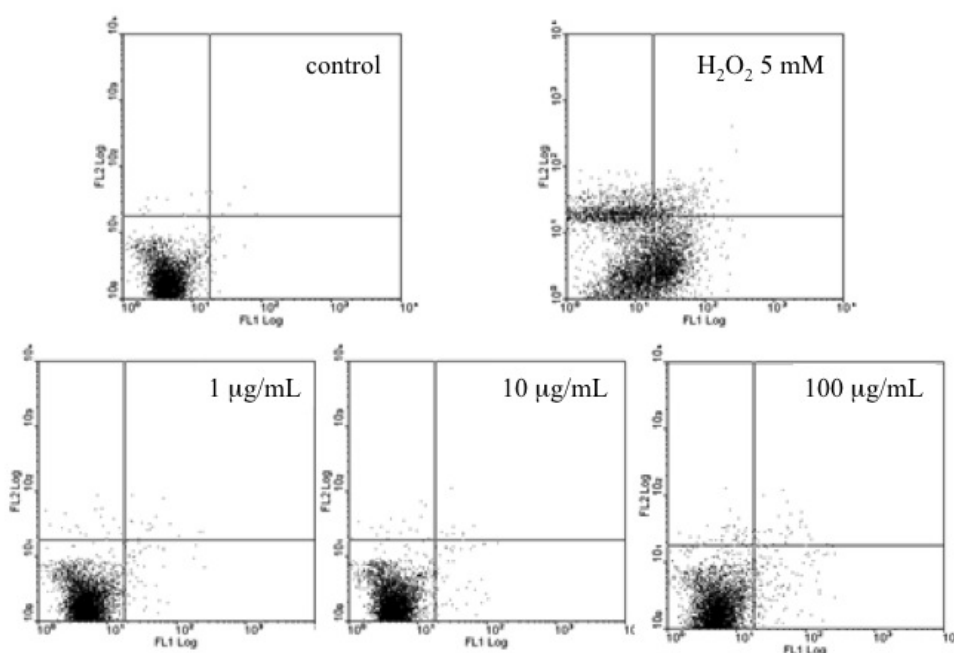
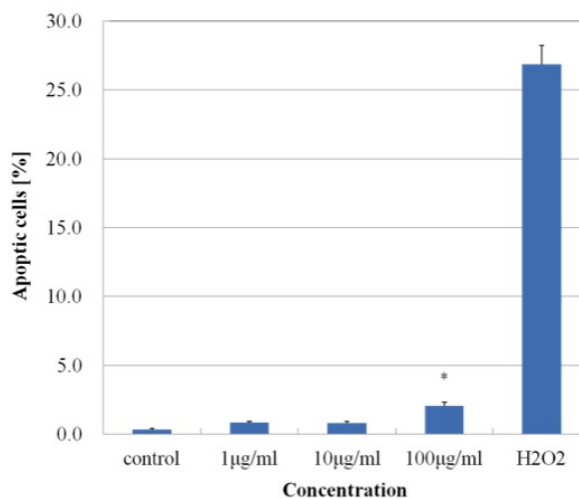


**Figure 5.** Effect of Fe<sub>3</sub>O<sub>4</sub> magnetic nanoparticles (MgNPs-Fe<sub>3</sub>O<sub>4</sub>) on apoptosis in A549 cells. A549 cells were treated with 0 (control), 1, 10 or 100 µg/mL MgNPs-Fe<sub>3</sub>O<sub>4</sub> for 24 h; cells were treated with 5 mM H<sub>2</sub>O<sub>2</sub> for 24 h as a positive control. Apoptosis of A549 cells treated with MgNPs-Fe<sub>3</sub>O<sub>4</sub> or H<sub>2</sub>O<sub>2</sub> was determined by flow cytometry based on propidium iodide/Annexin V staining patterns; **(a)** Representative flow cytometry of one set of triplicate experiments; **(b)** Percentages of apoptotic cells from flow cytometry analysis. Apoptotic cells include early apoptotic cells (AnnexinV+/PI-) and late apoptotic or necrotic cells (AnnexinV+/PI+). Data are presented as the mean ± SD of three independent experiments. \* *p* < 0.05 vs. control.

**(a)**



**(b)**



#### 2.4. Effect of MgNPs-Fe<sub>3</sub>O<sub>4</sub> on ROS Production, Intracellular Glutathione, and 8-OH-dG Levels in DNA

As shown in Figure 6, MgNPs-Fe<sub>3</sub>O<sub>4</sub> caused a dose-dependent increase in ROS production with concentrations of 10 and 100 µg/mL. Figure 7 demonstrates that MgNPs-Fe<sub>3</sub>O<sub>4</sub> caused a dose-dependent decrease in the GSH level; GSH was reduced by 65% with 100 µg/mL MgNPs-Fe<sub>3</sub>O<sub>4</sub>. The 8-OH-dG levels were increased approximately 8- and 14-fold above control with 10 and 100 µg/mL MgNPs-Fe<sub>3</sub>O<sub>4</sub>, respectively (Figure 8). ROS production by MgNPs-Fe<sub>3</sub>O<sub>4</sub> is well known to be involved in the cytotoxic response in various cell types. Fe<sub>3</sub>O<sub>4</sub>, a mixture of FeO and Fe<sub>2</sub>O<sub>3</sub>, is unstable and can readily undergo oxidation to yield  $\gamma$ -Fe<sub>2</sub>O<sub>3</sub> + Fe<sup>2+</sup> [7,9,16]. The free Fe<sup>2+</sup> ions can react with hydrogen peroxide and oxygen produced by the mitochondria to produce highly reactive hydroxyl radicals and Fe<sup>3+</sup> ions [17] that can damage DNA, proteins, polysaccharides, and lipids *in vivo*. Similar to our findings, previous studies have shown that Fe<sub>3</sub>O<sub>4</sub> elicited an increase in oxidative DNA lesions in A549 cells with minimal effect on cell viability [7–9]. Of the non-enzymatic antioxidants, GSH represents the major intracellular redox buffer in all cell types. Abundant in all cell compartments, it constitutes the first line of the cellular defense mechanism against oxidative injury [16]. Previous studies demonstrated that ROS generation following GSH depletion caused mitochondrial damage and up-regulation of pro-apoptosis mediators [2,7,18]. We found MgNPs also significantly reduced the GSH level. However, our data suggest that the shift in balance toward pro-oxidant mechanisms exerts little impact on cell viability.

**Figure 6.** Effect of MgNPs-Fe<sub>3</sub>O<sub>4</sub> on production of reactive oxygen species (ROS) by A549 cells. A549 cells were treated with doses 0 (control), 1, 10 or 100 µg/mL MgNPs-Fe<sub>3</sub>O<sub>4</sub> for 24 h. ROS production was determined using the CM-H<sub>2</sub>DCFDA assay. Data are presented as the mean ± SD of three independent experiments. \*\* *p* < 0.01 vs. control.

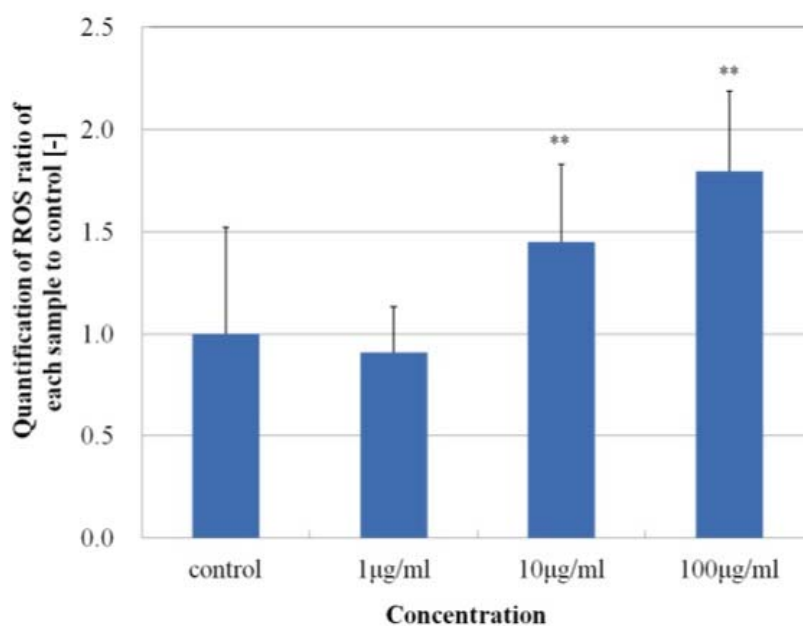


**Figure 7.** Effect of MgNPs-Fe<sub>3</sub>O<sub>4</sub> on intracellular glutathione (GSH) levels in A549 cells. A549 cells were treated with 0 (control), 1, 10 or 100 µg/mL MgNPs-Fe<sub>3</sub>O<sub>4</sub> for 24 h. GSH levels were assessed by luciferin bioluminescence (GSH-Glo Glutathione Assay Kit). Data are presented as the mean ± SD of three independent experiments. Significantly different from the untreated control at \*\*  $p < 0.01$  vs. control.

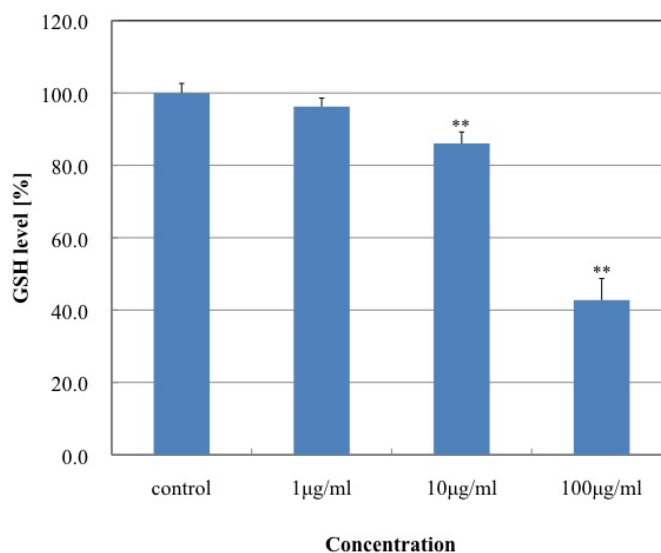
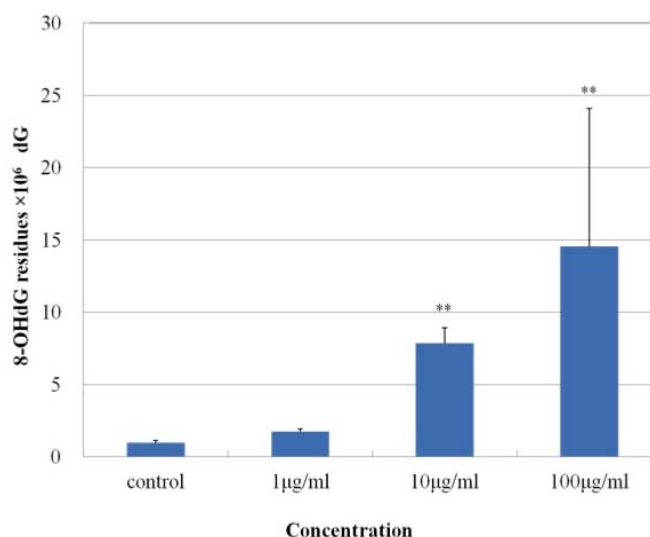


**Figure 8.** Effect of MgNPs-Fe<sub>3</sub>O<sub>4</sub> on 8-hydroxy-deoxyguanosine (8-OH-dG) levels in A549 cells. A549 cells were treated with 0 (control), 1, 10 or 100 µg/mL MgNPs-Fe<sub>3</sub>O<sub>4</sub> for 72 h. DNA was extracted by the sodium iodide method; 8-OH-dG levels were determined using HPLC-ECD. Data are presented as the mean ± SD of three independent experiments. \* Significantly different from the untreated control at \*\*  $p < 0.01$  vs. control.

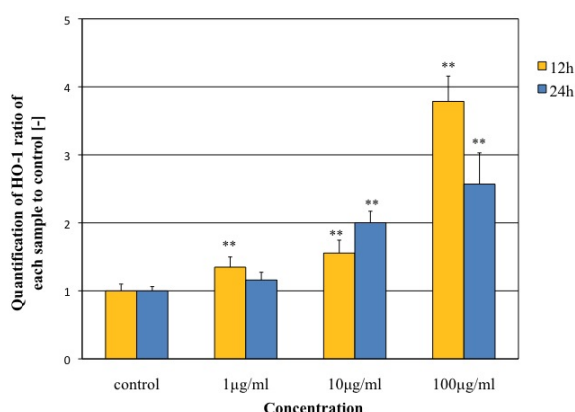


### 2.5. Expression of the Heme Oxygenase-1 (HO-1) Gene

As shown in Figure 9, the transcript level of the *HO-1* was induced in a dose-dependent manner after 12 and 24 h of MgNPs-Fe<sub>3</sub>O<sub>4</sub> exposure, however its transcription level at 100 mg/mL exposure after 24 h was reduced compared to after 12 h. Oxidative stress is caused by an imbalance in the level

of ROS and a biological system's ability to detoxify the reactive intermediates [16]. Cells possess both enzymatic and non-enzymatic mechanisms to counterbalance the cytotoxicity and genotoxicity caused by ROS [16]. In the lungs, the major enzymatic antioxidants are superoxide dismutases (SODs), catalase, and glutathione peroxidase (GSH-Px); others include those examined in this study, HO-1, thioredoxin (TR), and glutaredoxin (GLRX). HO-1 is involved in playing a major role in degradation of heme to biliverdin, but has recognized potent anti-inflammatory and anti-apoptotic effects [17,19]. HO-1 is induced mainly at the transcriptional level by oxidative stress, pro-inflammatory mediators, and some growth factors [18]. HO-1 mRNA expression is known to mediate antioxidant and cytoprotective effects and has been considered useful as a marker for particle-induced oxidative stress. Park *et al.* [20] showed that treatment of a human bronchial epithelial cell line with TiO<sub>2</sub>-MgNPs for four hours caused dose-dependent increases in mRNA expression of HOG-1, glutathione-S-transferase, and catalase; mRNA expression level of HO-1 had returned to baseline by 24 h [20]. Napierska *et al.* [21] also showed a marked induction of HO-1 mRNA in the endothelial cell at six hours after treatment of SiO<sub>2</sub>-NPs, but reduction of HO-1 mRNA at 24 h. Our results appear to be same as these two studies.

**Figure 9.** Effect of MgNPs-Fe<sub>3</sub>O<sub>4</sub> on mRNA expression of the *HO-1* gene in A549 cells. The expression level of the *HO-1* was normalized according to the expression level of  $\beta$ -actin. Data are presented as the mean  $\pm$  SD of three independent experiments. \*\*  $p < 0.01$  vs. control.

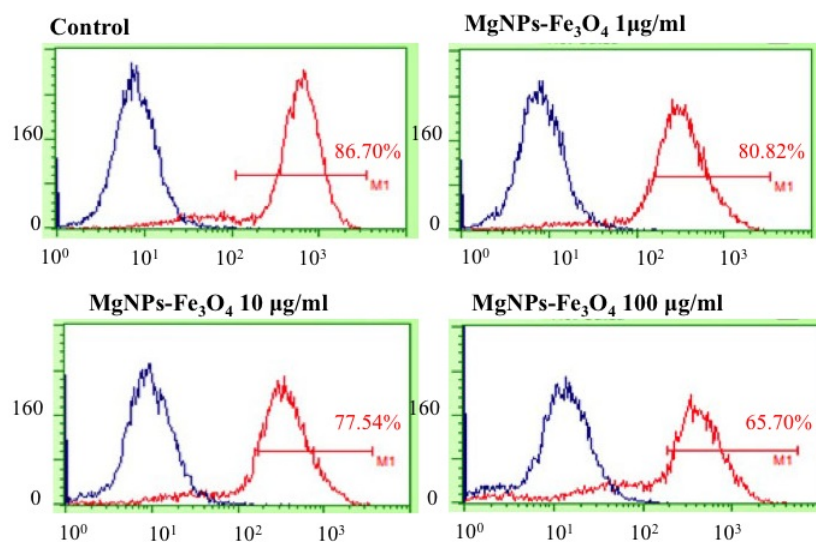


## 2.6. Effect of MgNPs-Fe<sub>3</sub>O<sub>4</sub> on CD44<sup>+</sup> Cell Fraction in A549 Cells

MgNPs-Fe<sub>3</sub>O<sub>4</sub> caused a dose-dependent reduction in the CD44<sup>+</sup> subpopulation (Figure 10). CD44 is a cell surface glycoprotein that mediates cellular adhesion to the extracellular matrix and is involved in multiple processes, including inflammation, cell migration, signaling, and tumor metastasis [13,22]. CD44 is up-regulated in the damaged epithelium of asthma patients, and is believed to be involved in tissue repair by localizing chemokines and growth factors to the disrupted epithelium [23]. CD44 is also a marker of certain cancer stem cells [24], in which it functions to defend cancer cells against oxidative stress by increasing GSH synthesis [25]. CD44 has also been reported to be involved in the protective effect of hyaluronate on constitutive DNA damage by ROS in A549 cells [26]. Consistent with the previously noted reduction in GSH and increase in 8-OH-dG levels, we found that MgNPs-Fe<sub>3</sub>O<sub>4</sub> markedly decreased the CD44<sup>+</sup> cell fraction of A549 cells. Thus, these results highlight another mechanism by which MgNPs-Fe<sub>3</sub>O<sub>4</sub> impair redox control and damage DNA in A549 cells. Our

results also offer the possibility that CD44 may be a marker MgNP-Fe<sub>3</sub>O<sub>4</sub>-induced cytotoxicity; however, further study is warranted.

**Figure 10.** Effect of Fe<sub>3</sub>O<sub>4</sub> magnetic nanoparticles (MgNPs-Fe<sub>3</sub>O<sub>4</sub>) on CD44<sup>+</sup> cell fraction in A549 cells. A549 cells were treated with 0 (control), 1, 10 or 100 µg/mL MgNPs-Fe<sub>3</sub>O<sub>4</sub> for 24 h. Cells were labeled with mouse anti-human CD44 monoclonal antibody; level of CD44<sup>+</sup> cells was determined by flow cytometry.



### 3. Experimental Section

#### 3.1. MgNPs-Fe<sub>3</sub>O<sub>4</sub>

MgNPs-Fe<sub>3</sub>O<sub>4</sub> were obtained from the Toda Kogyo Corporation (Otake, Hiroshima, Japan). As specified by the manufacturer, MgNPs in powder were spherical, with an average particle size of 10 nm, as measured by transmission electron microscopy (TEM), and a surface area of 100–120 m<sup>2</sup>/g. In suspension, the particle size ranged from 60 to 100 nm as measured by dynamic light scattering (DLS) and zeta potential ranged from –30 to –40 mV at pH 10. Bare MgNPs-Fe<sub>3</sub>O<sub>4</sub> were used in this study.

#### 3.2. Preparation of MgNPs-Fe<sub>3</sub>O<sub>4</sub> in Culture Medium

MgNPs-Fe<sub>3</sub>O<sub>4</sub> were sterilized by ultraviolet (UV) irradiation and suspended in phosphate-buffered saline (PBS), Ham's F-12 alone, and Ham's F-12 medium containing 10% fetal bovine serum (FBS) and 100 U/mL penicillin-streptomycin to yield a concentration of 1, 10 or 100 µg/mL. Suspensions were sonicated at 30 W for 10 min using an Ultrasonic HomogenizerVP-050 (TAITAEC, Koshigaya, Saitama, Japan).

#### 3.3. Cell Line

A549 human lung epithelial cells were purchased from American Tissue Type Culture Collection (Manassas, VA, USA). Cells were incubated in Ham's F-12 Medium with 10% fetal bovine serum

(FBS) and 100 U/mL penicillin–streptomycin in 5% CO<sub>2</sub> at 37 °C. Cells were maintained at a density of 60%–70% confluence in 100 mm dishes, and used in log-phase of growth.

### 3.4. Characterization of MgNP-Fe<sub>3</sub>O<sub>4</sub> Suspensions in Cell Culture Medium

The average hydrodynamic size and size distribution of MgNPs-Fe<sub>3</sub>O<sub>4</sub> in cell culture media and their intracellular localization were determined by DLS using a Fiber-Optics Particle Analyzer FPAR-1000 (Otsuka Electronics, Hirakata, Osaka, Japan). MgNPs-Fe<sub>3</sub>O<sub>4</sub> were suspended in Ham's F-12 Medium with or without 10% FBS and supplements, or in phosphate-buffered saline (PBS).

### 3.5. Cellular Uptake of MgNPs-Fe<sub>3</sub>O<sub>4</sub> in A549 Cells

The cellular uptake of MgNPs-Fe<sub>3</sub>O<sub>4</sub> in A549 cells was analyzed as follows.

#### 3.5.1. Transmission Electron Microscopy (TEM)

A549 cells were fixed with 3% glutaraldehyde in 0.1 M cacodylate buffer (pH 7.3) at 4 °C for 4 h. Samples were post-fixed with 2% osmium tetroxide at 4 °C for 2 h, dehydrated, and embedded in epoxy resin. Ultrathin sections (80 nm) were then stained with uranyl acetate and lead citrate, and observed by TEM.

#### 3.5.2. Flow Cytometry Assay

A549 cells were treated with 0, 1, 10 or 100 µg/mL MgNPs-Fe<sub>3</sub>O<sub>4</sub> for 24 h, and then trypsinized and suspended in medium. Cellular uptake of MgNPs-Fe<sub>3</sub>O<sub>4</sub> was analyzed using flow cytometry (Millipore, Billerica, MA, USA), in which the intensities of forward-scattered (FS) and side-scattered (SS) light are proportional to cell size and intracellular density of MgNPs-Fe<sub>3</sub>O<sub>4</sub>, respectively. A total of 30,000 cells were measured per sample.

### 3.6. AlamarBlue Assay

Cell viability was determined using the alamarBlue assay (Alamar Biosciences, Sacramento, California, USA) according to the manufacturer's instructions. Briefly, cells ( $1.0 \times 10^4$  cells/well) were incubated with MgNPs-Fe<sub>3</sub>O<sub>4</sub> (0, 1, 10 or 100 µg/mL) for 72 h at 37 °C. AlamarBlue (10%) was added to each well and incubated for 200 min. Metabolically active cells reduced the dye to a fluorescent form, which was measured using a plate reader (excitation/emission: 570 nm/600 nm; Viento XS, DS Pharma Biomedical, Suita, Osaka, Japan). Cell viability was determined by linear interpolation of the emission from cells treated with 0.1% saponin (0% viability) and untreated cells (100% viability).

### 3.7. Lactate Dehydrogenase (LDH) Release Assay

LDH release assay to assess membrane integrity was performed using LDH-cytotoxicity assay kit (BioVision, CA, USA) according to the manufacturer's instructions. Cells cultured in 24-well plates ( $1.5 \times 10^4$  cells/well) were treated with 0, 1, 10 or 100 µg/mL MgNPs-Fe<sub>3</sub>O<sub>4</sub> for 24 h at 37 °C. Plates were then centrifuged at  $250 \times g$  for 5 min. The supernatant of each well was transferred to a fresh, flat

bottom 96-well culture plate containing 100  $\mu$ L reaction mixture, and incubated for 30 min at room temperature. Formazan absorbance—an index of the number of lysed cells—was measured by a microplate reader at 500 nm (Viento XS, DS Pharma Biomedical, Osaka, Japan).

### 3.8. Apoptosis by Flow Cytometry (FCM)

A549 cells ( $1.0 \times 10^6$  cells) were cultured on 100-mm culture dishes, and treated with 0, 1, 10 or 100  $\mu$ g/mL MgNPs-Fe<sub>3</sub>O<sub>4</sub> for 24 h at 37 °C. Cells were harvested, washed gently with PBS, collected by centrifugation, and then stained using an Annexin V-FITC Kit (Beckman Coulter, Marseille, France) following the manufacturer's instructions. Cells were stained with Annexin V and propidium iodide (PI, Sigma-Aldrich, St. Louis, MO, USA), and analyzed by flow cytometry (Becton Dickinson, Franklin Lakes, NJ, USA) within 1 h of staining using the FL1 (FITC) and FL3 (PI) lines.

### 3.9. Measurement of Intracellular Reactive Oxygen Species (ROS)

ROS were measured using the CM-H<sub>2</sub>DCFDA assay (Invitrogen, Carlsbad, CA, USA) according to the manufacturer's instructions. Cells ( $1.0 \times 10^4$  cells/well) in 24 well-plates were treated with 0, 1, 10 or 100  $\mu$ g/mL MGNPs-Fe<sub>3</sub>O<sub>4</sub> for 24 h at 37 °C. A fresh stock solution of 5 mM CM-H<sub>2</sub>DCFDA was prepared in DMSO and diluted to a final concentration of 1  $\mu$ M in PBS. Cells were washed with PBS, followed by incubation with 50  $\mu$ L of working solution of the fluorochrome marker CM-H<sub>2</sub> DCFDA for 30 min. Fluorescent images were obtained using an IX2N-FL-1 microscope (Olympus, Tokyo, Japan), and analyzed using imaging soft (Photoshop Elements 8, Adobe systems, Tokyo, Japan). The data were expressed as percentage of the unexposed control.

### 3.10. Intracellular Reduced Glutathione (GSH) Assay

Intracellular GSH level was determined using a GSH-Glo Glutathione assay kit (Promega, Madison, WI, USA) according to the manufacturer's instructions. Briefly, cells were seeded in 96-well plates and treated with 0, 1, 10 or 100  $\mu$ g/mL MgNPs-Fe<sub>3</sub>O<sub>4</sub> for 24 h at 37 °C. The cells were washed with DPBS, and the GSH-Glo reagent was added to each well for 30 min at room temperature to allow the cells to convert a luciferin derivative into luciferin. Reconstituted luciferin detection reagent was then added to each well for 15 min, and the luminescent signal was measured with a Glomax multi detection system (Promega, Madison, WI, USA).

### 3.11. Analysis of 8-Hydroxy-2'-Deoxyguanosine (8-OH-dG) in DNA

A549 cells were incubated with 0, 1, 10 or 100  $\mu$ g/mL MGNPs-Fe<sub>3</sub>O<sub>4</sub> for 72 h at 37 °C (5% CO<sub>2</sub>). The nuclear DNA was isolated by the sodium iodide method. The 8-OH-dG levels were analyzed by HPLC-ECD methods as previously described [27]. The amount of 8-OH-dG in the DNA was determined by comparison to authentic standards, and expressed as the number of 8-OH-dG per 10<sup>6</sup> deoxyguanosine (dG) residues.

### 3.12. Oxidative Stress-Related Gene Expression Analysis

A549 cells were treated with 0, 1, 10, or 100 µg/mL MgNPs-Fe<sub>3</sub>O<sub>4</sub> for 24 h at 37 °C. Total RNA was isolated using ISOGEN (Nippon Gene, Tokyo, Japan), and cDNA was produced using a mixture containing Superscript RNase H Reverse Transcriptase (Invitrogen, Carlsbad, CA, USA), oligo dT primer, and 2.5 mmol/L dNTP. Quantitative real-time PCR was conducted using the LINE GENE real-time PCR detection system (BioFlux, Tokyo, Japan) with the SYBR Premix Ex Taq Perfect Real Time Kit (Takara Bio. Inc., Otsu, Japan). The PCR reaction consisted of initial thermal activation at 95 °C for 10 s and 40 cycles. Each cycle was as follows: 95 °C for 5 s; 60 °C for 26 s. PCR products were verified by analysis of heat-dissociation curves and amplification plots. Quantitative values were acquired from linear regression of the PCR standard curve. The primer sequences of the amplified genes are as follows [28,29]; *Heme oxygenase-1*, forward 5'-GGTGATAGAAGAGGCCAAGAC-3' and reverse 5'-GCAGAATCTTGCACTTTGTTG-3', *β-actin*, forward 5'-GGATGCAGAAGGAGATCACTG-3' and reverse 5'-CGATCCACACGGAGTACTTG-3'.

### 3.13. Immunostaining and Flow Cytometric Analysis for CD44<sup>+</sup> Cell Fraction

A549 cells were treated with 0, 1, 10 or 100 µg/mL MgNPs-Fe<sub>3</sub>O<sub>4</sub> for 24 h at 37 °C. Cells were then labeled in a PBS solution with a mouse anti-human CD44 monoclonal antibody conjugated with fluorescein isothiocyanate (clone SFF-2, Millipore, Billerica, MA, USA) for 1 h at room temperature. A mouse IgG immunoglobulin and dye conjugate IgG was used as control for non-specific binding. Flow cytometric analysis was performed with a Guava-EasyCyte\*HT using Guava Express Pro software (Millipore, Billerica, MA, USA) gating for CD44<sup>+</sup> cells. A minimum of 10,000 cells was measured per sample.

### 3.14. Statistical Analysis

Data are presented as the mean ± standard deviation (SD). Differences between treated and untreated control cells were determined using one-way ANOVA followed by Dunnett's test. Differences were considered statistically significant at  $p < 0.05$ .

## 4. Conclusions

MgNPs-Fe<sub>3</sub>O<sub>4</sub> up to a concentration of 100 µg/mL exerted minimal effect on viability of A549 cells, despite causing a significant reduction in antioxidant capacity and an increase in oxidative damage to DNA. Increased expression of an oxidative stress-related gene was not sufficient to prevent the decrease in GSH content. The decrease in the CD44<sup>+</sup> cell fraction was consistent with the observed drop in GSH concentration and increase in 8-OH-dG level.

## Acknowledgments

This research was supported in part by a Grant-in-Aid for the Global COE Program from the Ministry of Education, Culture, Sports, Science and Technology of Japan, a Grant-in-Aid for Research

on Risk of Chemical Substances from the Ministry of Health, Labour and Welfare of Japan, and a Research Grand-in-Aid from Magnetic Health Science Foundation.

### Conflict of Interest

The authors report no conflict of interest. The authors are responsible for the content and writing of the paper.

### References

1. Chakraborty, M.; Jain, S.; Rani, V. Nanotechnology: Emerging tool for diagnostics and therapeutics. *Appl. Biochem. Biotechnol.* **2011**, *165*, 1178–1187.
2. Ramesh, V.; Ravichandran, P.; Copeland, C.L.; Gopikrishnan, R.; Biradar, S.; Goornavar, V.; Ramesh, G.T.; Hall, J.C. Magnetite induces oxidative stress and apoptosis in lung epithelial cells. *Mol. Cell. Biochem.* **2012**, *363*, 225–234.
3. Parveen, S.; Misra, R.; Sahoo, S.K. Nanoparticles: A boon to drug delivery, therapeutics, diagnostics and imaging. *Nanomedicine* **2012**, *8*, 147–166.
4. Hilger, I.; Kaiser, W.A. Iron oxide-based nanostructures for MRI and magnetic hyperthermia. *Nanomedicine* **2012**, *7*, 1443–1459.
5. Chen, B.; Sun, Q.; Wang, X.; Gao, F.; Dai, Y.; Yin, Y.; Ding, J.; Gao, C.; Cheng, J.; Li, J.; *et al.* Reversal in multidrug resistance by magnetic nanoparticle of Fe<sub>3</sub>O<sub>4</sub> loaded with adriamycin and tetrandrine in K562/A02 leukemic cells. *Int. J. Nanomed.* **2008**, *3*, 277–286.
6. Sato, A.; Itcho, N.; Ishiguro, H.; Okamoto, D.; Kawai, K.; Kasai, H.; Kurioka, D.; Uemura, H.; Kubota, Y.; Watanabe, M. Magnetic nanoparticles of Fe<sub>3</sub>O<sub>4</sub> enhance docetaxel-induced prostate cancer cell death. *Int. J. Nanomed.* **2013**, in press.
7. Singh, N.; Jenkins, G.J.; Asadi, R.; Doak, S.H. Potential toxicity of superparamagnetic iron oxide nanoparticles (SPION). *Nano Rev.* **2010**, *1*, 5358.
8. Karlsson, H.L.; Cronholm, P.; Gustafsson, J.; Möller, L. Copper oxide nanoparticles are highly toxic: A comparison between metal oxide nanoparticles and carbon nanotubes. *Chem. Res. Toxicol.* **2008**, *21*, 1726–1732.
9. Kim, J.E.; Shin, J.Y.; Cho, M.H. Magnetic nanoparticles: An update of application for drug delivery and possible toxic effects. *Arch. Toxicol.* **2012**, *86*, 685–700.
10. Lewinski, N.; Colvin, V.; Drezek, R. Cytotoxicity of nanoparticles. *Small* **2008**, *4*, 26–49.
11. Klein, S.; Sommer, A.; Distel, L.V.; Neuhuber, W.; Krysch, C. Superparamagnetic iron oxide nanoparticles as radiosensitizer via enhanced reactive oxygen species formation. *Biochem. Biophys. Res. Commun.* **2012**, *425*, 393–397.
12. Holgate, S.T. Epithelial damage and response. *Clin. Exp. Allergy.* **2000**, *1*, 37–41.
13. Kitamura, H.; Okudela, K.; Yazawa, T.; Sato, H.; Shimoyamada, H. Cancer stem cell: Implications in cancer biology and therapy with special reference to lung cancer. *Lung Cancer* **2009**, *66*, 275–281.
14. Hong, S.C.; Lee, J.H.; Kim, H.Y.; Park, J.Y.; Cho, J.; Lee, J.; Han, D.W. Subtle cytotoxicity and genotoxicity differences in superparamagnetic iron oxide nanoparticles coated with various functional groups. *Int. J. Nanomed.* **2011**, *6*, 3219–3231.

15. Wiogo, H.T.R.; Lim, M.; Bulmus, V.; Yun, J.; Amal, R. Stabilization of magnetic iron oxide nanoparticles in biological media by fetal bovine serum (FBS). *Langmuir* **2011**, *27*, 843–850.
16. Birben, E.; Sahiner, U.M.; Sackesen, C.; Erzurum, S.; Kalayci, O. Oxidative stress and antioxidant defense. *World Allergy Organ J.* **2012**, *5*, 9–19.
17. Tulis, D.A.; Durante, W.; Liu, X.; Evans, A.; Peyton, K.J.; Schafer, A.I. Adenovirus-mediated heme oxygenase-1 gene delivery inhibits injury-induced vascular neointima formation. *Circulation* **2001**, *104*, 2710–2715.
18. Morita, T. Heme oxygenase and atherosclerosis. *Thromb. Vasc. Biol.* **2005**, *25*, 1786–1795.
19. Durante, W. Heme oxygenase-1 in growth control and its clinical application to vascular disease. *J. Cell Physiol.* **2003**, *195*, 373–382.
20. Park, E.J.; Yi, J.; Chung, K.H.; Ryu, D.Y.; Choi, J.; Park, K. Oxidative stress and apoptosis induced by titanium dioxide nanoparticles in cultured BEAS-2B cells. *Toxicol. Lett.* **2008**, *180*, 222–229.
21. Napierska, D.; Rabolli, V.; Thomassen, L.C.J.; Dinsdale, D.; Princen, C.; Gonzalez, L.; Poels, K.L.C.; Kirsch-Volders, M.; Lison, D.; Martens, J.A.; *et al.* Oxidative stress induced by pure and iron-doped amorphous silica nanoparticles in subtoxic conditions. *Chem. Res. Toxicol.* **2012**, *25*, 828–837.
22. Yasuda, M.; Nakano, K.; Yasumoto, K.; Tanaka, Y. CD44: Functional relevance to inflammation and malignancy. *Histol. Histopathol.* **2002**, *17*, 945–950.
23. Leir, S.H.; Baker, J.E.; Holgate, S.T.; Lackie, P.M. Increased CD44 expression in human bronchial epithelial repair after damage or plating at low cell densities. *Am. J. Physiol. Lung Cell Mol. Physiol.* **2000**, *278*, L1129–L1137.
24. Leung, E.L.; Fiscus, R.R.; Tung, J.W.; Tin, V.P.; Cheng, L.C.; Sihoe, A.D.; Fink, L.M.; Ma, Y.; Wong, M.P. Non-small cell lung cancer cells expressing CD44 are enriched for stem cell-like properties. *PLoS One* **2010**, *5*, e14062.
25. Nagano, O.; Okazaki, S.; Saya, H. Redox regulation in stem-like cancer cells by CD44 variant isoforms. *Oncogene* **2013**, in press.
26. Zhao, H.; Tanaka, T.; Mitlitski, V.; Heeter, J.; Balazs, E.A.; Darzynkiewicz, Z. Protective effect of hyaluronate on oxidative DNA damage in WI-38 and A549 cells. *Int. J. Oncol.* **2008**, *32*, 1159–1167.
27. Kawai, K.; Li, Y.S.; Kasai, H. Accurate measurement of 8-OH-dG and 8-OH-Gua in mouse DNA, urine and serum: Effects of X-ray irradiation. *Genes Environ.* **2007**, *29*, 107–114.
28. Miyake, M.; Fujimoto, K.; Anai, S.; Ohnishi, S.; Kuwada, M.; Nakai, Y.; Inoue, T.; Matsumura, Y.; Tomioka, A.; Ikeda, T.; *et al.* Heme oxygenase-1 promotes angiogenesis in urothelial carcinoma of the urinary bladder. *Oncol. Rep.* **2011**, *25*, 653–660.
29. Wang, C.; Tian, Y.; Lei, B.; Xiao, X.; Ye, Z.; Li, F.; Kijlstra, A.; Yang, P. Decreased IL-27 expression in association with an increased Th17 response in Vogt-Koyanagi-Harada disease. *Invest. Ophthalmol. Vis. Sci.* **2012**, *53*, 4668–4675.